Possible mechanism for aligning microscopic flexible filaments predicted using "caterpillar" hydrodynamics

A. G. Bailey and C. P. Lowe

Possible mechanism for aligning microscopic flexible filaments predicted using "caterpillar" hydrodynamics

A. G. Bailey

Haas School of Business,

University of California,

Berkeley CA 94720, USA

C. P. Lowe

Van 't Hoff Institute for Molecular Sciences (HIMS)

University of Amsterdam

PO Box 94157, 1090 GD Amsterdam

Netherlands

Abstract

We use the "caterpillar" hydrodynamic model for accurately calculating the hydrodynamic friction force on microscopic slender cylindrical filaments using Oseen level hydrodynamics. The methodology is applied to study the motion of a flexible filament in a circularly polarized field. Our results predict that in dilute solution alignment occurs along the axis of the field. For electric fields, the strengths and frequencies required are deduced. These are experimentally accessible. We therefore propose that this is a practical method for aligning filaments such as microtubules and functionalized carbon nanotubes.

I. INTRODUCTION

Many slender microscopic filaments display remarkable properties. Notable examples are carbon nanotubes and biological fibers, such as actin and microtubules. In cells, the latter provide both strength and a means of intracellular transport. They act as "tracks" along which nano-scale motor proteins process, transporting cargo such as vesicles and large proteins. An intriguing possibility is that of mimicking this system for use in microfluidic devices [1]. With the emergence of engineered devices at microscale and nanoscale dimensions, there is a need for controlled transport at these length scales and the kinesin-microtubule system provides a highly evolved biological transport system well adapted for these tasks [2]. The ability to manipulate their orientation is a fundamental requirement for this. That is, imparting directionality to an otherwise disordered system. This is not straightforward. Focusing on microtubules, their electrostatic/dynamic properties can be exploited for alignment. In experiments using AC fields with high strengths and frequencies, induced dipole alignment (parallel to the field) has been demonstrated [3, 4]. The magnitude of the induced dipole, and hence susceptibility to alignment, depends on the ionic strength, pH, and field frequency and magnitude. On surfaces, alignment can be achieved by using kinesin and polarity-specific antibodies for immobilization prior to the application of external fields [5, 6].

Alternatively, as well as the fact that they are charged, one can also exploit the fact that filaments are normally dispersed in a viscous environment. Moths and Witten [7, 8] showed that for rigid asymmetric colloidal particles this can lead to alignment. Flexibility also influences their behavior [9–12]. Notably, if slender filaments are subject to a force that generates translational motion (gravity or an electric field, for example) they will tend to orientate in a plane perpendicular to that force. The origin of this effect is the interplay between hydrodynamic friction, which varies along the length as a function of distance from the ends, and bending elasticity. In short, when one allows for the force mediated by the fluid on different parts of the filament, the friction it experiences is higher towards the ends, causing it to bend. This bending in turn introduces a force anisotropy in the form of a torque leading to rotation and a re-orientation into the perpendicular plane. Note that this differs from the effect described in references [7, 8] in that, unlike the asymmetric rigid model, in the rigid limit the variation of the friction along the filament here is symmetric. It is the bending that breaks the symmetry so in the limit of a rigid filament there is no asymmetry

2

and the reorientation time tends to infinity [11]. Within the plane there is no alignment and uniform translational motion will also induce significant inhomogeneity in the system. The question we address here is: is there some other way of exploiting this flexibility effect that can actually align filaments to a particular direction? Specifically, we consider a filament in a circularly polarized field. Such a field conveniently avoids net translation, but does the elasto-hydrodynamic aligning effect persist? If so, how does the filament quantitatively respond to such a field? To answer these questions we use computer simulation. Our first requirement is a numerical model that accurately captures the relevant effects.

II. DESCRIPTION OF THE MODEL

Given the complexity of the interplay between varying hydrodynamic forces and the deformation of even a single flexible filament, analytic solutions are few [13]. This is particularly true outside the linear regime. We have therefore constructed a tractable but sufficiently sophisticated numerical model to solve the problem by firstly considering a filament of length L discretized into n beads. The distance between neighboring beads is fixed, meaning that the model filament is inextensible, and the bead separation is given by $b = L/(n-1)$. As the filament deforms elasticity will penalize deviation from the lowest energy conformation. The Hamiltonian of our model system is derived by introducing a bending potential between all sets of three consecutive beads and assuming that there is no intrinsic curvature (see Ref. [11, 14]). The inextensibility constraint is imposed using the MILC SHAKE algorithm [15]. Filaments of fixed length are effectively infinitely stiff while retaining flexibility. The reason we chose this approach is that the type of filaments we consider cannot accommodate significant axial extension. Experiments support that this is a reasonable description of force-extension behavior [16, 17]. The most technical part of the problem is determining the force exerted on the filament by the surrounding fluid, given that the movement of the filament itself perturbs the fluid. Since the filaments we are considering are microscopic in length, it is reasonable to neglect inertial effects. In this limit the fluid flow equations are linear. An approximate approach couples the filament and fluid motion by requiring that beads in the model act as Stokeslets (point forces acting in the fluid)[18]. They experience a hydrodynamic frictional force given by

$$\mathbf{F}_H = -\left(\gamma_0^\perp \hat{\mathbf{n}}\hat{\mathbf{n}} + \gamma_0^\parallel \hat{\mathbf{p}}\hat{\mathbf{p}}\right) \cdot (\mathbf{v} - \mathbf{v}_H) \qquad (1)$$

where $\mathbf{v}$ is the velocity of the bead and $\mathbf{v}_H$ is the induced fluid velocity at its location. The vector $\hat{\mathbf{n}}$ ($\hat{\mathbf{p}}$) is the unit vector normal (parallel) to the axis. The parameters $\hat{\gamma}_0$ are then the bead friction coefficients. In this model the local fluid velocity $\mathbf{v}_H$ is now a linear combination of the velocity fields generated at that point by each of the Stokeslets [11, 19, 20], leading to a hydrodynamic force on bead i given by

$$\mathbf{F}_{iH} = - \left(\gamma_0^{\perp} \hat{\mathbf{n}} \hat{\mathbf{n}} + \gamma_0^{\|} \hat{\mathbf{p}} \hat{\mathbf{p}} \right) \cdot$$
$$\left(\mathbf{v}_i - \frac{1}{8\pi\eta} \sum_{i \neq j} \left(\frac{\mathbf{F}_j}{|\mathbf{r}_{ij}|} + \mathbf{F}_j \cdot \frac{\mathbf{r}_{ij}\mathbf{r}_{ij}}{|r_{ij}|^3} \right) \right). \tag{2}$$

The constants $\hat{\gamma}_0$ can also be written in terms of the friction exerted by a sphere of radii $\hat{a}$, $\gamma_0^{\perp(\|)} = 6\pi\eta a^{\perp(\|)}$, where the constant η is the viscosity. Note that $\hat{a}$ are not "real" radii, in that the beads in the model have no spacial extension. Rather, they are parameters determining the friction strength. The question is now, what values to take for $\hat{a}/b$? One choice is the "shish kebab" model, where $a^{\perp}/b = a^{\|}/b = 1/2$. However, Bailey et $al.$ [21] showed that for this model the friction coefficient of the filament for motion perpendicular and parallel to the axis ($\gamma^{\perp}$ and $\gamma^{\|}$) are

$$\gamma^{\perp} = \frac{4\pi\eta L}{ln\left(L/\beta b\right) + \frac{2b}{3a^{\perp}} - 1} + O\left(ln^{-3}(L/\beta b)\right) \tag{3}$$

$$\gamma^{\|} = \frac{2\pi\eta L}{\ln\left(L/(\beta b)\right) + \frac{b}{3a} - 1} + O\left(ln^{-3}(L/\beta b)\right) \tag{4}$$

where $\beta = e^{-k}$ and k is the Euler-Mascheroni constant. The theoretical result from slender body theory is also of this form, but the constants in the denominators depend on the shape of the filament [22]. Only when the perpendicular hydrodynamic radius is chosen to be $a^{\perp}/b = 4/(3(2\ln(2)+1)) \approx 0.559$ is this model in agreement with theory to the order of error in the equations. This value is close to, but not equal to, the shish kebab value. Similarly, the parallel friction coefficient matches theory when the parallel hydrodynamic radius is chosen to be $a^{\|}/b = 2/(3(2\ln(2)-1)) \approx 1.73$ (still with $r/b = \beta$). This differs more significantly from the shish kebab value and also differs from the perpendicular radius. The agreement of the Stokeslet (or "caterpillar") model with theoretical results is thus conditional upon choosing the hydrodynamic radius, and hence bead friction coefficient, to be the tensor

$$\gamma_0^{\perp} = 6\pi\eta a^{\perp} = 8\pi\eta b \left(2\ln(2) + 1\right)^{-1}$$
$$\gamma_0^{\|} = 6\pi\eta a^{\|} = 4\pi\eta b \left(2\ln(2) - 1\right)^{-1}. \tag{5}$$

4

We also note that this methodology is equally applicable to match to numerical expressions for the friction, instead of slender body theory results. These may be preferable for filaments with lower aspect ratios. Here we restrict ourselves to slender filaments. In this limit, a similar analysis shows that only with these choices of hydrodynamic radii is the correct *variation* of the friction coefficient along the length of the filament recovered to $O(\ln^{-3}(\epsilon))$ in the slenderness parameter $\epsilon = r/l$. This is crucial, because it is this variation in friction along the length that causes a flexible filament to bend when it is set in motion and this is the origin of the effect we are considering here. Higher order hydrodynamic approximations are possible for modeling a filament. For example, the Rotne-Prager (RP) tensor [23]. These have the advantage of removing singularities in the Oseen tensor that give rise to large errors when two beads come into close contact. For the work reported here we do not consider the close approach of two filaments. The divergence in the Oseen tensor causes no problems, so using a higher order tensor would simply introduce an unnecessary computational overhead.

III. RESULTS

We now turn to investigating the possibility of aligning filaments using a circularly polarized field. This could be a gravitational field or an electric field. As discussed in ref. [11], it is difficult in experiments (although not impossible) to access the regime where gravitational fields are high enough to induce significant bending. Consequently, we restrict ourselves to analyzing regimes easily accessed using an electric field. Microtubules are charged biofilaments that have been shown to respond to moderate, experimentally accessible electric fields [9, 12]. Carbon nanotubes, on the other hand, are uncharged but can be functionalized to give an effective electrical charge [24]. One could question whether a hydrodynamic model based on the Oseen tensor is valid for the particular case of a charged filament because there exists the possibility that the presence of counter ions screens this tensor [25]. However, the experiments of van den Heuvel *et al.* [12] convincingly showed that for microtubules the induced bending followed scaling behaviour consistent with a hydrodynamic mechanism. Because this mechanism is itself a consequence of the long range nature of the hydrodynamic propagator, this observation strongly suggests that for filaments any such screening is either absent or incomplete.

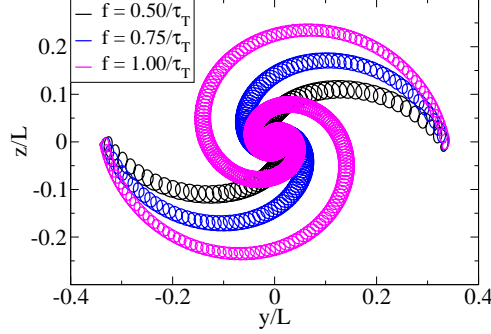We carried out a series of simulations using the model described above in experimentally

FIG. 1: A trace of the ends of the filament during alignment process after subtracting the center of mass motion for three different field frequencies ($B = 1.2$).

accessible regimes of parameter space. The purely dissipative equations of motion were solved in the limit of negligible inertia. We apply an electric field of the form $E_x = 0$, $E_y = E\cos{(2\pi f t)}\,\hat{y}$, $E_z = E\sin{(2\pi f t)}\,\hat{z}$, where E and f are the field magnitude and frequency, respectively. In all cases we set $L = 1$ and the number of beads in the model to 80. In the caterpillar model the number of beads fixes the aspect ratio. For this value, its accuracy is shown in [21]. Following the argument above, we are then considering a cylindrical filament with aspect ratio $L/d \sim 80$ (although the effect considered here only depends logarithmically on the aspect ratio [21]). For a microtubule (diameter 25 nm), this would typically correspond to a length of a couple of microns. We define a dimensionless force $B = L^3 E\tilde{q}/\alpha$ that characterizes the magnitude of the electric forces to the elastic forces. Here, $\tilde{q}$ is the charge density of the filament, and α is the flexure. The effect of flexibility enters through B. When $B \gg 1$, significant deformation is expected, whereas when $B \ll 1$ elastic forces dominate and the filament will remain predominantly straight. The rigid case is the limit $B \to 0$. We can estimate experimentally accessible values of B for microtubules. From Ref. [9], the average length L was 5 μm, the flexure α is of the order 10 $pN\mu m^2$, and the effective linear charge density was measured to be $\tilde{q} = 280$ $e/\mu m$. The microtubules remained stable in a field of 20 V/cm. Using these values, we calculate that $B \sim 1$ is easily achieved experimentally. Experiments carried out by van den Heuvel *et al.* actually achieved much higher values, and pronounced bending was indeed observed [12]. In our simulations B is near the modest value of unity. We also define a characteristic time $\tau_T = \bar{\gamma}^{\perp}/E\tilde{q}$, which is the amount of time it takes the filament experiencing an external field

of magnitude E to translate transversely a distance of its length.

The simulations predict that a charged body placed in circularly-polarized field gyrates in the yz-plane following the direction of the applied field. The center of mass motion occurs concurrently with a hydrodynamic re-orientation due to bending of the filament. Traces of the location of the endpoints of the filament after subtracting the center of mass motion for representative simulations are shown in Fig. 1. Here, the filament is initially tilted at an angle of 45 degrees in the xy-plane, but in time it aligns itself with $\hat{x}$, perpendicular to the plane of the polarized field [26]. There is also an azimuthal angle to consider, but this only influences the initial direction of motion (i.e. rotates results shown in Fig. 1). Our results suggest that circularly polarized electric fields are a indeed a possible means for aligning charged filaments. Before we can propose that the method is also *practical* there are other things to consider.

The filament motion resembles sedimentation constrained to the surface of a cylinder. If the radius of this cylinder is too large then there is pronounced rotational motion, which is undesirable. The magnitude of this steady state gyration radius R can be estimated using simple scaling arguments. We expect $2\pi R \sim \omega/f$, where ω is the tangential velocity. When the frequency of the electric field is chosen to be $f = \tau_T^{-1}$ and $\omega = L/\tau_T$, $R \sim L/2\pi$, independent of B the field strength. This expression is exact for $B \to 0$, where bending is insignificant. We further confirmed from simulations, with a dimensionless force ranging from $B = 0.08 - 1.6$, that the expression for R remains sufficiently accurate for values of B around unity to provide a reasonable estimate for the spatial extension of the rotation of the filament during the alignment process. From this we can conclude that, so long as the frequency is around τ_T^{-1} or higher, the rotation can be localized to lengths of the order of the length of the filament.

To now quantify the time scale of re-orientation, we define the hydrodynamic alignment time τ_H as the time taken for the angle between the filament axis and $\hat{x}$ to decrease by ten degrees. This is somewhat arbitrary, but one would reach the same conclusions for the scaling behavior with a different definition of the change required to define τ_H. The first parameter we consider is the magnitude of the frequency of the applied field. In the limit where $f \ll \bar{\tau}_H^{-1}$, where $\bar{\tau}_H$ is the hydrodynamic alignment time in a static field ($f = 0$), we recover the results discussed in Ref. [11]. As we increase the frequency while keeping B constant, the alignment time increases. This dependence is shown in Fig. 2. The filament spends an
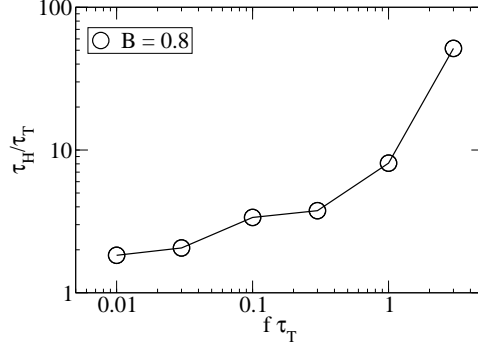
FIG. 2: Hydrodynamic alignment time, τ_H, as a function of frequency (B = 0.8).
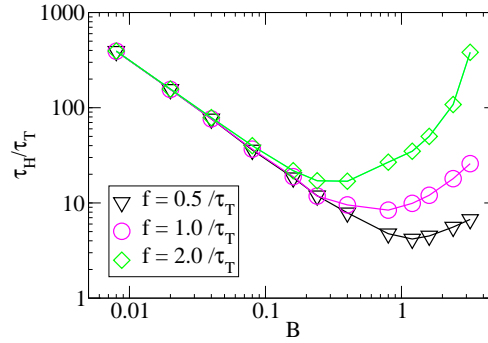

FIG. 3: Hydrodynamic alignment time, τ_H, as a function of the dimensionless field strength, B.

increased amount of time changing orientation to adjust to the alternating direction of the field. The result is that when the frequency is too high, the filament takes an impractically long amount of time to align. So long that the effect of diffusion cannot be ignored and a deterministic simulation is no longer valid (see below). When the frequency is approximately τ_T^{-1} then, for $B \sim 1$, the alignment time is (using values for microtubules reported in Ref. [9]) a modest $\tau_T \sim 1\ s$.

The dependence of τ_H on the dimensionless field strength B is shown in Fig. 3. One can observe two scaling regimes. For low B's, the observed relationship is $\tau_H \sim \gamma^\perp / \tilde{F} B$, which is consistent with that observed in Ref. [11] for alignment in a static field. One can predict this by noting the analytical expression for the torque from Ref. [27] scales with $\sim \tilde{F} B$. Since the rigid case is the limit $B \to 0$, we see that, as for the case of sedimentation, the alignment time in this limit approaches infinity. For high B's, the hydrodynamic alignment time obeys a different scaling relationship: τ_H actually increases with B. This is because

the frequency for these simulations is chosen to be proportional to τ_T^{-1}, so as B increases, so does the frequency and therefore the alignment time, as discussed in the previous paragraph. The crossover of scaling behavior therefore occurs when $f \sim \bar{\tau}_H^{-1}$. Using the shish kebab parameterization leads to qualitatively the same conclusion, but differs quantitatively by some 30%. So for a direct comparison with possible experiments the difference between the shish kebab and caterpillar is significant.

Other forces are present that will compete with the hydrodynamic forces driving alignment. As long as τ_H is shorter than all other time scales, hydrodynamic re-orientation will dominate these effects. First, thermal forces act to randomize its orientation. The time scale for rotational diffusion is roughly $\tau_D \sim \gamma^\perp L^2/kT$. We can neglect this when $\tau_H/\tau_D \sim L/B^2\lambda \ll 1$, where λ is the persistence length ($\lambda = \alpha/kT$). For a 5 μm microtubule, this condition is satisfied as long as $B > 0.1$. Additionally, under certain conditions microtubules in solution have an induced dipole moment along their axis [3, 4, 9]. The time scale associated with the alignment of the dipole with the field can be estimated by $\tau_d \sim \gamma^\perp L^2/d_{el}E$. To ensure that this process is negligible requires that $\tau_H/\tau_d \sim d_{el}/\tilde{q}BL^2 \ll 1$, where $d_{el} \sim \bar{\alpha}EL$ and $\bar{\alpha}$ is the effective polarization coefficient per unit length of the microtubule [4]. This leads to the condition that for $B \sim 1$, $\bar{\alpha}E/\tilde{q}L \ll 1$. Therefore, the influence of the induced dipole can be minimized by increasing the filament length and by changing the solvent conditions and external field parameters to minimize $\bar{\alpha}$ [3, 4, 12]. I

A final complication is the presence of other filaments. We considered the scenario of two filaments separated by a distance h, exposed to the same field described above. At the start of the simulation, one filament is aligned with the $\hat{x}$ direction, and the second is tilted at an angle of 60 degrees in the xy-plane. The alignment time was measured for multiple separations. In the regime where $h/L > 1$, the filaments behave as isolated entities. This is consistent with the results from studies of cooperative motion in a static field carried out by Llopis *et al.* [28]. For $h/L < 1$, a more complicated dynamic is observed that is strongly dependent on the initial conditions. Therefore we cannot immediately conclude whether alignment is hindered or assisted in concentrated solutions, given the wide range of parameter space. It suffices to say as that as long as the solution is at a low enough concentration, neighboring filaments should do not inhibit alignment.

IV. CONCLUSIONS

To conclude, our simulations predict that it is practical to align flexible charged filaments in dilute solution to a prescribed direction using a circularly polarized field. For the case of an electric field we delineate the window of parameter space for achieving this alignment. These predictions assume that the hydrodynamic interaction of the filament with itself is not screened. Any deviations from the predictions of the simulations would therefore shed light on the important open question as to how the presence of counter ions influence the forces acting on a charged filament. We hope that this will motivate experimental studies and ultimately provide a useful tool for technological applications.

V. ACKNOWLEDGEMENTS

[1] M. G. L. van den Heuvel and C. Dekker, Science **317**,333 (2007).

[2] J. L. Malcos and W.O Hancock, Appl. Microbiol. Biotechnol. **90**, 1 (2011).

[3] K. Bohm, N. Mavromatos, A. Michette, R. Stracke, and E. unger, Electromagn. Biol. Med. **24**, 319 (2005).

[4] I. Minoura and E. Muto, Biophys. J. **90**, 3739 (2006).

[5] L. Limberis, J. J. Magda, and R. J. Stewart, Nano Lett. **1**, 277 (2001).

[6] M. E. Williams, B. M. Hutchins, M. Platt and W. O. Hancock ECS Transactions, **3**, 1 (2007).

[7] B. Moths and T. A. Witten, Phys. Rev. Lett. **110**, 028301 (2013).

[8] B. Moths and T.A. Witten, Phys. Rev. **E88**, 022307 (2013).

[9] R. Stracke, K. Bohm, L. Wollweber, J. Tuszynski, and E. Unger, Biochem. Biophys. Res. Commun. **293**, 602 (2002).

[10] M. Tanase, L. Bauer, A. Hultgren, D. Silevitch, L. Sun, D. Reich, P. Searson, and G. Meyer, Nano Lett. **1**, 155 (2001).

[11] M. Cosentino-Lagomarsino, I. Pagonabarraga, and C. P. Lowe, Phys. Rev. Lett. **94**, 148104 (2005).

[12] M. van den Heuvel, R. Bondesan, M. Cosentino-Lagomarsino, and C. Dekker, Phys. Rev. Lett. **101**, 118301 (2008).

[13] B. Chakrabarti and J.A. Hanna, J. Fluids Struct. **66**, 490 (2016).

[14] C. Lowe, Phil. Trans. Roy. Soc. London **358**, 1543 (2003).

[15] A. G. Bailey, C. P. Lowe, and A. P. Sutton, J. Comput. Phys. **227**, 8949 (2008).

[16] S. B. Smith, L. Finzi, and C. Bustamante, Science **258**, 1122 (1992).

[17] J. Marko and E. Siggia, Macromolecules **28**, 8759 (1995).

[18] G. Stokes, Trans. Camb. Phil. Soc. **9**, 8 (1851).

[19] Y. Kim and R. Netz, Phys. Rev. Lett. **96**, 158101 (2006).

[20] X. Schlagberger and R. Netz, Phys. Rev. Lett. **98**, 128301 (2007).

[21] A.G. Bailey, C.P. Lowe, I. Pagonabarraga and M. Cosentino-Lagomarsino, Phys. Rev. bf E 80, 046707 (2009).

[22] R. G. Cox, J. Fluid Mech. **44**, 791 (1970).

[23] J. Rotne and S. Prager, J. Chem. Phys. **50**, 4831 (1969).

[24] K. Balasubramanian and M. Burghard, Small **1**, 180 (2005).

[25] D. Long and A. Ajdari, Eur. Phys. J. **E 4**, 29 (2001).

[26] An animation of the typical dynamics can be viewed at http://www.cmth.ph.ic.ac.uk/people/aimee.bailey/movie.mov (also *.avi).

[27] X. Xu and A. Nadim, Phys. Fluids **6**, 2889 (1994).

[28] I. Llopis, I. Pagonabarraga, M. Cosentino-Lagomarsino, and C. P. Lowe, Phys. Rev. E **76**, 061901 (2007).